JOURNAL OF Materials CHEMISTRY

Tetraalkyl- and dialkyl-substituted BEDT-TTF derivatives and their cation-radical salts: synthesis, structure, and properties

Aravinda M. Kini,* James P. Parakka, Urs Geiser, Hsien-Hau Wang, Felix Rivas, Ernest DiNino, Seddon Thomas, James D. Dudek and Jack M. Williams

Chemistry and Materials Science Divisions, Argonne National Laboratory, 9700 South Cass Avenue, Argonne, Illinois, 60439-4831, USA

Received 23rd November 1998, Accepted 23rd December 1998

Tetraalkyl and dialkyl derivatives, where alkyl = ethyl and propyl, of the organic electron donor molecule bis(ethylenedithio)tetrathiafulvalene, BEDT-TTF or ET, have been synthesized *via* the Diels–Alder approach. Several cation-radical salts of these new donors have been prepared and structurally characterized, and found to contain donor molecules in nominally higher oxidation states (+1, +1.5 and +2) than the typically observed oxidation state of +0.5 in BEDT-TTF salts. The higher solubility of the tetraalkyl and dialkyl derivatives in solvents used for crystal growth is proposed as the principal reason for this finding. Surprisingly, X-ray crystallographic studies reveal that the alkyl groups in the neutral tetraethyl-ET as well as the oxidized tetraethyl-ET and diethyl-ET molecules in their cation-radical salts adopt axial configurations, rather than the expected equatorial configurations. Electrical properties of the cation-radical salts have been found to be either insulating or semiconducting, consistent with the higher oxidation states of the donor molecules in the salts and the crystal structures.

Introduction

There is unabated interest in the design and synthesis of suitable molecular precursors for the preparation of organic metals and superconductors.[1] One of the key requirements for the realization of superconductivity in organic cation-radical salts is the ability of the constituent organic donor molecules to engage in intermolecular π–π overlaps in two (or higher) dimensions leading to two-dimensional (or higher) band electronic structures, thus precluding the metal–insulator or metal–semiconductor transitions ubiquitous in systems of lower electronic dimensionality.[2] This is the principal driving force behind the discovery of more than 50 superconducting cation-radical salts based on the prototypic BEDT-TTF or ET electron-donor molecule.[3] Several new electron-donor molecules which incorporate the features of the ET molecule (*e.g.*, a large number of sulfur or other heteroatoms along the periphery of highly conjugated molecules) have recently been reported.[4] An alternative molecular design strategy that holds considerable promise is to append substituents and/or additional heterocyclic rings to the ET skeleton, in anticipation of these addenda dominating intermolecular interactions, and leading to new molecular packing patterns conducive to two-dimensional electronic structures.[5] Our recent work on the syntheses of ET derivatives with appended 1,4-dioxane rings[6] and aromatic rings (benzo, naphtho)[7] was based on the premise that the intermolecular CH···O interactions in the former and aromatic π–π interactions in the latter would lead to new packing motifs and new two-dimensional materials. An additional motivation in the work above was to increase the thickness of the non-conducting layer in the cation-radical salts with a layered structure, so that the empirical relationship between the thickness of the non-conducting layer and superconducting transition temperatures (T_c), T_c being inversely correlated with the thickness, could be further substantiated.[6] In the present work, we have extended this line of reasoning to include *n*-alkyl groups with their well-known hydrophobic interactions (attractive in nature) influencing the molecular packing modes, and have synthesized ET derivatives with ethyl and *n*-propyl substituents. These derivatives are also of interest to us in the design and synthesis of 'molecular rulers'.[8] The syntheses of the corresponding methyl derivatives of ET, both dimethyl and tetramethyl derivatives, have been previously reported.[5a,9] In 1992, Zambounis *et al.* reported the discovery of a superconducting salt of the dimethyl-ET derivative, κ-(*S*,*S*-dimethyl-ET)$_2$ClO$_4$, $T_c \approx 3$ K (5 kbar).[10]

The attachment of alkyl substituents to ethane-1,2-diyl endgroups of the ET molecule results in chiral carbon centers, and consequently, for multiply substituted ET derivatives, several stereoisomers are possible. The substituents can be in either *cis* or *trans* configurations, and for each of the configurations they can be in either axial or equatorial conformations. Furthermore, two sets of diastereomers arise from the relative stereochemistry of the two halves of the molecule. When both halves are the same (either *cis* or *trans*), a *meso*-form and an enantiomeric pair are possible. In order to minimize the number of stereoisomers, and more importantly, to minimize unfavorable packing interactions, we focused on the ET derivatives in which each ethanediyl moiety has alkyl substituents in a *trans* configuration. It was further expected that the *trans* alkyl substituents will adopt equatorial conformations, so that face-to-face and side-by-side π–π overlaps between the donor molecules will be possible in the solids derived from these derivatives, akin to the case of the parent ET molecule.

In this paper, we describe the synthesis of *trans*,*trans*-tetraalkyl-ET (alkyl = ethyl and *n*-propyl) and *trans*-diethyl-ET *via* the Diels–Alder cycloaddition reaction of the trithione oligomer with appropriate *trans*-alkenes, their crystal structures, and the preparation, structure and properties of several

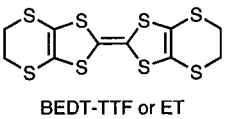

BEDT-TTF or ET

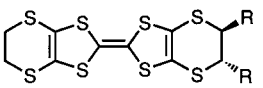

R = Et Diethyl-ET

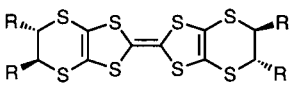

R = Et Tetraethyl-ET
R = n-Pr Tetrapropyl-ET

cation-radical salts derived from these new electron-donor molecules.

Results and discussion

Synthesis

The early work by Neilands *et al.*[11] and Khodorkovsky *et al.*[12] on the synthesis of the trithione oligomer, and its ability to undergo Diels–Alder reaction with alkenes, has been extended by several groups recently toward the synthesis of several TTF derivatives.[13] However, as far as we were aware, all the alkenes reported in these reactions were either monosubstituted or cyclic, and not disubstituted alkenes.[14] We reasoned that *trans*-disubstituted alkenes might provide a convenient access to the required intermediates for our target compounds. On the other hand, the dimethyl and tetramethyl derivatives of ET were synthesized *via* the nucleophilic substitution reaction of 1,3-dithiole-2-thione-4,5-dithiolate (dmit) with cyclic sulfate diester derived from optically active (*R*,*R*)-butane-2,3-diol or (*S*,*S*)-butane-2,3-diol.[5a,9] As an alternative, we have exploited the stereospecific nature of the [4+2] cycloaddition between the trithione oligomer and *trans*-alkenes to provide the required intermediate thiones expeditiously and in high yields, albeit as racemic mixtures.

The reaction of the oligo(trithione) with *trans*-hex-3-ene and *trans*-oct-4-ene in refluxing toluene furnished the thiones **3a** and **3b** in 77% and 73% yields respectively after purification. While the *trans* stereochemistry in the adducts cannot be unambiguously determined from the spectral data, from the X-ray structural studies of the final TTF derivative **5a** (*vide infra*), *trans* stereochemistry is suggested for the cycloadducts. ^{1}H NMR spectra of compounds **3a** and **3b** reveal a complex multiplet (13 lines) for the methine protons, which suggests a racemic mixture of both (*R*,*R*) and (*S*,*S*) diastereomers. This is entirely consistent with the equal probability for the approach of *trans*-alkene towards the trithione in two orientations.

The thiones **3a** and **3b** were converted to the corresponding carbonyl derivatives **4a** and **4b** by use of mercuric acetate in 72% and 68% yields (after recrystallization) respectively. Trimethyl phosphite-mediated self-coupling of **4a** and **4b** furnished the tetraethyl-ET (**5a**) and tetra(*n*-propyl)-ET (**5b**) in 74% and 70% yields respectively (Scheme 1).

The unsymmetrical ET derivative, diethyl-ET (**7**), was also synthesized with the object of reducing the number of possible stereoisomers. Trimethyl phosphite mediated cross-coupling reaction of **6** and **4a** afforded **7**, along with byproducts ET (**8**) and **5a** resulting from the homocoupling reaction (Scheme 2). Different experimental conditions employed for the formation of **7** along with the product yields are tabulated in Table 1. The yield of **7** was further improved to *ca.* 35% by reacting the known dithiocarbonate **9** with the trithiocarbonate **3a** in refluxing trimethyl phosphite, *i.e.*, by use of starting materials in which the thiocarbonyl and carbonyl functionalities are switched (Scheme 2).

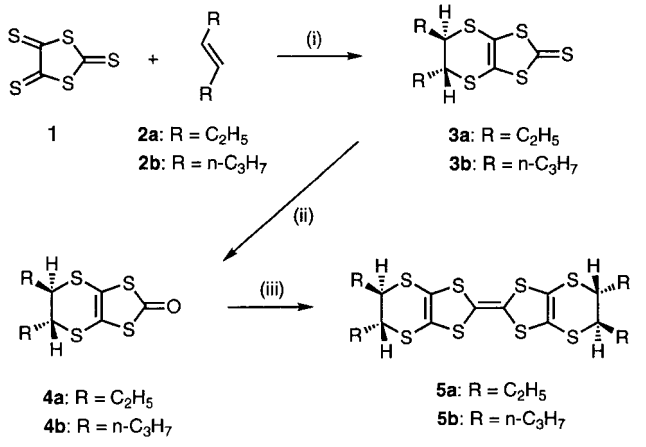

Scheme 1 *Reagents and conditions*: (i) Toluene, reflux; (ii) $Hg(OAc)_2$, chloroform : acetic acid (4 : 1), rt; (iii) $(MeO)_3P$, reflux.

Electrochemistry

The redox properties of the electron donor molecules prepared in this study were determined by use of cyclic voltammetry, and are summarized in Table 2. All the new ET derivatives displayed two reversible redox waves with half-wave potentials very similar to those of ET, recorded under identical experimental conditions. Appending four alkyl groups on the dithiine rings of ET appears to decrease the oxidation potentials only marginally in comparison to the oxidation potentials of ET (**8**). The unsymmetrical ET derivative **7**, containing two ethyl groups, in accord with expectations, exhibited oxidation potentials intermediate between those of ET and the tetraethyl derivative **5a**.

Preparation of cation-radical salts

Preparation of the cation-radical salts of the newly synthesized ET derivatives, **5a**, **5b** and **7**, was attempted by use of both chemical oxidation and electrocrystallization techniques. The three electron-donor molecules were found to be considerably more soluble than ET in solvents commonly used for the crystallization of the cation-radical salts, such as 1,1,2-trichloroethane (TCE), tetrahydrofuran (THF) and dichloromethane. Consequently, our attempts to prepare crystals of cation-radical salts have been unsuccessful thus far in the case of tetrapropyl-ET (**5b**), and have met with limited success in the case of tetraethyl-ET (**5a**) and diethyl-ET (**7**). Crystal growth by electrocrystallization was successful in the case of **5a** when $AuCl_4^-$, IBr_2^- and ClO_4^- were used as the electrolytes, and by chemical oxidation when I_2 vapor was used as the oxidant (see Experimental section for details).

The isolated cation-radical salt of **5a** when $AuCl_4^-$ was used as the electrolyte was found to be (**5a**)$(AuCl_4)(AuCl_2)$ by X-ray diffraction studies (see below). The anion portion of the salt consists of two monovalent anions in which gold is present in +3 and +1 oxidation states. The $[Au(I)Cl_2]^-$ ion evidently originates from the reduction of $[Au(III)Cl_4]^-$ ion, a fairly good oxidant, by the electron-donor molecule **5a** during the electrocrystallization process. In fact, when a solution of $(Ph_4P)Au(III)Cl_4$ in TCE is mixed with a solution of **5a** in TCE, an immediate dark coloration is observed, suggesting the spontaneous occurrence of such a redox reaction. The formal charge of 2+ on the electron-donor molecule is unusual but not unprecedented.[15,16] An ET salt of similar composition and stoichiometry has been previously reported.[15]

Electrocrystallization of **5a** in THF with $(Bu_4N)IBr_2$ as the electrolyte resulted in the isolation of a salt with the composition (**5a**)$(IBr_2)_2$, as determined by X-ray diffraction studies (see below). The formation of the 1 : 2 salt, in which the electron-donor **5a** is in the +2 oxidation state, is again noteworthy. On the other hand, chemical oxidation of **5a** in TCE by slow diffusion of iodine vapor resulted in the isolation of a salt of 1 : 1 stoichiometry with the composition (**5a**)$(I_3)(solvent)_x$. This salt is not very stable, and on standing at room temperature for over a month slowly loses iodine, reverting back to the orange colored neutral donor **5a**. Hence, the crystal structure determination (data collection over a few hours) was carried out on freshly prepared crystals.

The perchlorate salt of **5a** was obtained by electrocrystallization using tetrabutylammonium perchlorate as the electrolyte and chlorobenzene as the solvent. The crystals of this salt were too small for X-ray structure determination, but its composi-

Table 1 Reaction conditions and product yields

Starting materials	Reaction conditions	Product yields (%)		
		7	**8**	**5a**
6+**4a**	18 equiv. $(MeO)_3P$, reflux	24	17	10
6+**4a**	7 equiv. $(MeO)_3P$, toluene, reflux	14	5	2
6+**4a**	7 equiv. $(MeO)_3P$, $(MeO)_3P{=}O$, 105–108 °C	24	9	9
9+**3a**	17 equiv. $(MeO)_3P$, reflux	35	23	11

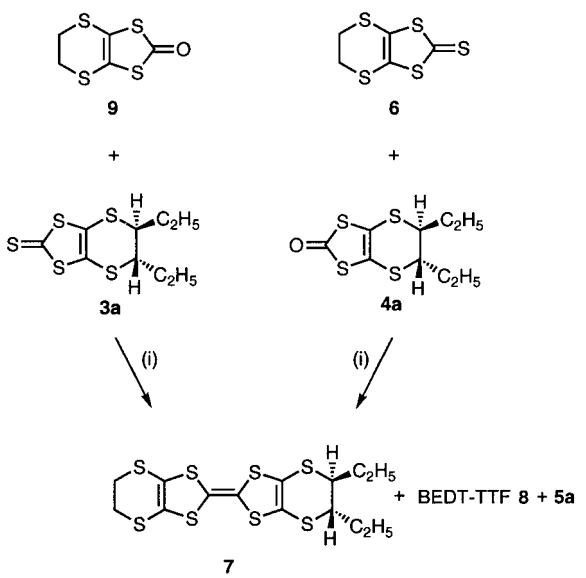

Scheme 2 *Reagents and conditions*: (i) $(MeO)_3P$; see Table 1 for varied conditions and yields.

Table 2 Electrochemical half-wave potentials[a] of the ET derivatives

Donor molecule	Half-wave potentials/V *vs.* $Ag/AgNO_3$	
	$E_{1/2}{}^1$	$E_{1/2}{}^2$
ET (**8**)	0.08	0.49
Tetraethyl-ET (**5a**)	0.01	0.43
Tetrapropyl-ET (**5b**)	0.03	0.44
Diethyl-ET (**7**)	0.05	0.47

[a]Potentials recorded using a Pt disk working electrode, Pt wire as counter electrode, and Ag/0.1 M $AgNO_3$ in CH_3CN as reference electrode at a scan rate 100 mV s^{-1}, employing dichloromethane as solvent containing 0.1 M *n*-Bu_4NPF_6 electrolyte.

tion was established to be 1:1, *i.e.*, (**5a**)ClO_4, from Raman spectroscopy (*vide infra*).

The cation-radical salt $(\mathbf{7})_2(IBr_2)_3$, of the unsymmetrical donor molecule diethyl-ET (**7**), was prepared by electrocrystallization using tetrabutylammonium dibromoiodate as the electrolyte in THF.

Crystal structures

All crystal structures were determined at room temperature by use of a Siemens SMART CCD-area detector single crystal X-ray diffractometer. Graphite-monochromatized MoKα radiation ($\lambda = 0.7107$ Å) was utilized, and essentially complete hemispheres to 0.75 Å resolution were collected on 0.3° ω-scan exposures. Crystal data are listed in Table 3. Full crystallographic details, excluding structure factor tables, have been deposited at the Cambridge Crystallographic Data Centre (CCDC). For details of the deposition scheme, see 'Instructions for Authors', *J. Chem. Soc., Perkin Trans. 1*, available *via* the RSC web page (http://www.rsc.org/authors). Any request to the CCDC for this material should quote the full literature citation and the reference number 1145/138. See http://www.rsc.org/suppdata/jm/1999/883/ for crystallographic files in cif format.

(*rac*-5a). The well-formed orange blocks were found to contain the racemate of the D_2-symmetric, optically active isomer. Despite the presence of both optically active isomers, they occupy distinct crystallographic sites, and the overall structure is chiral. The crystal selected for the analysis had the space group $P4_32_12$, but it is likely that the crystallization product contains equal amounts of spontaneously resolved $P4_12_12$ and $P4_32_12$ crystals. The crystal structure contains spiraling ribbons of molecules, with four molecules per *c*-axis repeat distance, see Fig. 1. Short (3.52 Å and 3.54 Å) S···S contacts connect the neighboring molecules. When projected along the long molecular axis (Fig. 1 bottom), the molecules at the vertices (Mol. 1) are of *R*,*R*′;*R*,*R*′-symmetry, whereas those on the nodes (Mol. 2) are of *S*,*S*′;*S*,*S*′-symmetry. A

Table 3 Crystal data at ambient temperature, 298(2) K, for neutral **5a** and its cation-radical salts, as well as for $(\mathbf{7})_2(IBr_2)_3$

	5a	(**5a**)$(AuCl_2)(AuCl_4)$	(**5a**)$(IBr_2)_2$	(**5a**)$I_3(TCE)_x$	$(\mathbf{7})_2(IBr_2)_3$
a/Å	13.9032(5)	18.619(2)	13.190(3)	39.754(2)	35.639(2)
b/Å	13.9032(5)	19.864(2)	18.925(4)	13.8902(7)	9.4278(4)
c/Å	23.9326(12)	8.4853(8)	6.5035(13)	11.4853(6)	14.7617(7)
α (°)	90	90	90	90	90
β (°)	90	90	98.19(3)	92.722(1)	94.456(1)
γ (°)	90	90	90	90	90
V/Å^3	4626.2(3)	3138.3(5)	1606.8(6)	6445.0(6)	4944.9(4)
Z	8	4	2	8	4
Space group	$P4_32_12$	*Cmcm*	*C*2/*m*	*C*2/*c*	$P2_1/c$
Mw	496.85	1111.55	1070.29	925.52[a]	1741.66
ρ_{calc}/g cm^{-3}	1.427	2.353	2.212	1.941[a]	2.339
μ/cm^{-1}	7.7	103.9	74.6	35.8[a]	74.5
$R(F_o)(F_o > 4\sigma)$	0.050	0.059	0.050	0.086	0.076
$wR(F_o^2)$ (all refs)	0.100	0.123	0.125	0.189	0.187

$R(F_o) = \Sigma|F_o - F_c|/\Sigma|F_o|$
$wR(F_o^2) = [\Sigma w(F_o^2 - F_c^2)^2/\Sigma w(F_o^2)^2]^{1/2}$
[a]Assuming $x = 1$.

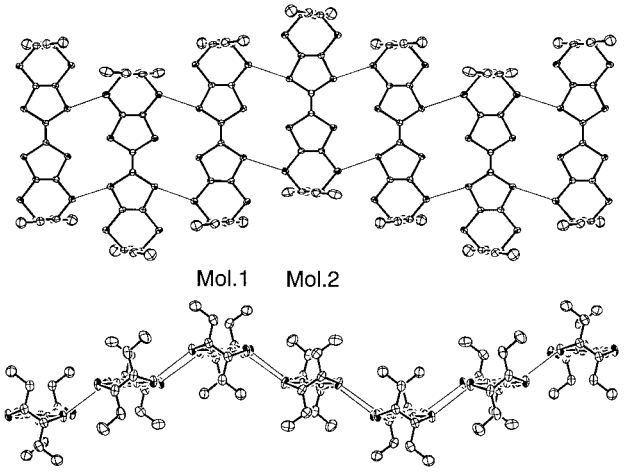

Fig. 1 Top and side view of the spiraling ribbons in neutral **5a**. Hydrogen atoms are omitted for clarity, and intermolecular S···S contacts less than the sum of the van der Waals radii (3.6 Å) are indicated with thin lines. The *c*-axis is horizontal.

crystallographic two-fold rotation axis intersects Mol. 1 perpendicular to the molecular plane. A different two-fold rotation axis is located along the central C=C bond of the molecule at site 2. Adjacent ribbons are rotated by 90° around the ribbon axis and shifted by one-quarter repeat distance. All molecules were found to possess their ethyl groups in the axial, and not in the expected equatorial positions, see Fig. 2. This result is in sharp contrast to the situation in tetramethyl-ET; in both neutral tetramethyl-ET (*R*,*R*′;*R*,*R*′ configuration)[9b] and its cation-radical salt with PF_6^- counterion,[9a] the methyl groups were found in the equatorial positions. Interestingly, in the dimethyl-ET derivative with *R*,*R*′ configuration, the methyl groups were found in the axial position.[9b] Given the well-documented conformational mobility of the endgroups in the ET molecule and its methyl derivatives (as probed by variable temperature NMR[9b]), these findings suggest the importance of molecular packing interactions being the deciding factor in whether the axial or equatorial conformer is incorporated in the crystals.

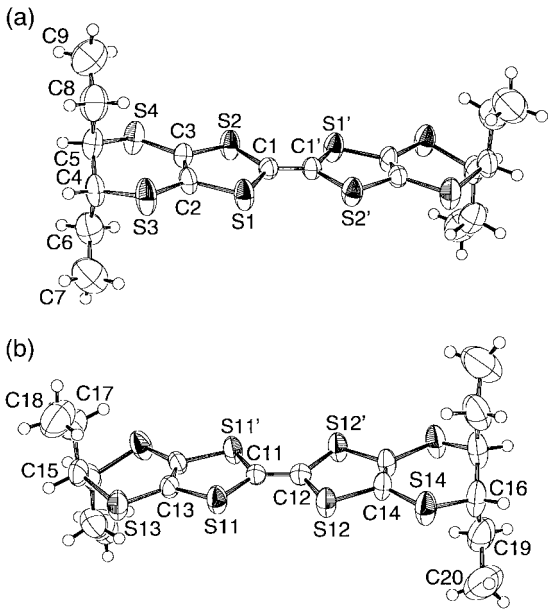

Fig. 2 The two crystallographically independent molecules in neutral **5a** with atomic labels of the unique atoms. Some equivalent atoms (indicated by primes) are labeled as well. All atoms except hydrogen (not labeled) are drawn with 50% probability thermal ellipsoids.

(5a)(AuCl$_2$)(AuCl$_4$). The site symmetry of the electron donor molecule in the dichloroaurate(I)/tetrachloroaurate(III) mixed-anion salt is C_{2v}, with crystallographic mirror planes perpendicular to the planar portion of the molecule (*ac*-plane). Therefore, a disordered model, consisting of a superposition of all possible ethyl group arrangements, had to be refined for the ethylene endgroups and the ethyl substituents, and the crystallographic information cannot distinguish between the isomers, see Fig. 3. Refinement of an ordered model (*meso*-form) in the non-centrosymmetric space group $Cmc2_1$ did not improve the agreement factors, and the residual electron density also indicated ethyl group disorder. As shown in Fig. 4, neighboring electron donors form zigzag ribbons in the *c*-direction, with $AuCl_2^-$ anions filling the 'pockets' of the zigzag ribbon. Short intermolecular contacts exist between sulfur and chlorine atoms, but adjacent donor molecules are too distant (>4 Å interatomic distances) for any significant orbital overlap among the cations to occur. The donor cations are capped on one side by the $AuCl_2^-$ anions and on the other by $AuCl_4^-$ anions, see Fig. 4.

(*meso*-5a)(IBr$_2$)$_2$. The electron donor molecule found in the dibromoiodate salt of **5a** is located on a C_{2h} crystallographic special position (two-fold rotation axis along central C=C bond), thus the isomer is the *meso*-form, or *R*,*R*′;*S*,*S*′. There is no indication of any significant isomeric disorder or scrambling. The fundamental building block of the crystal structure is a side-by-side association (ion triplet) of one electron donor molecule dication with two anions, with S···I and S···Br contacts that are significantly shorter than the

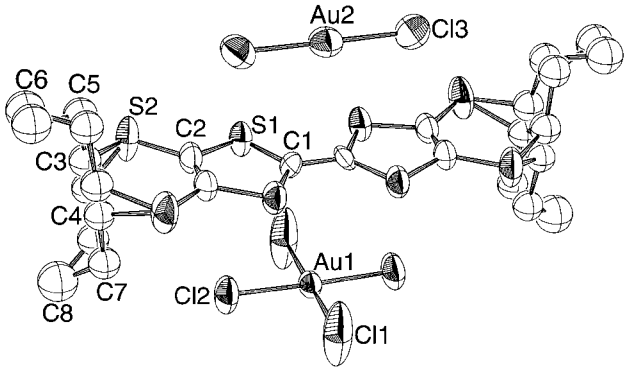

Fig. 3 Disordered model of the electron donor molecule and its neighboring anions in (**5a**)(AuCl$_4$)(AuCl$_2$) with atomic labels of the unique atoms. Hydrogen atoms were omitted from the calculations and are not shown, whereas all other atoms are drawn with 50% probability thermal ellipsoids.

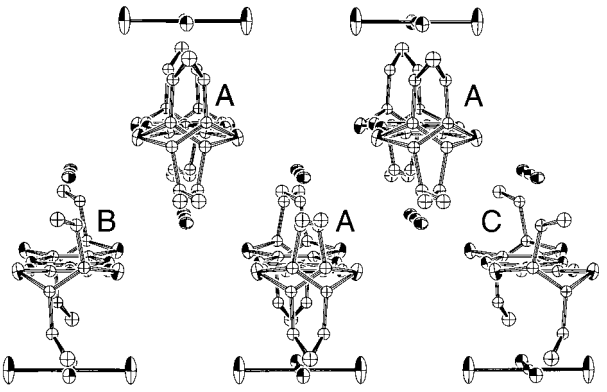

Fig. 4 Molecular packing (**5a**)(AuCl$_4$)(AuCl$_2$) as viewed approximately along the *a*-direction. The *c*-axis is horizontal. Donor molecules labeled A are drawn with their ethylene groups disordered, whereas molecules B and C are shown in two of the possible isomeric configurations. Hydrogen atoms are omitted for clarity.

sum of the van der Waals radii (3.78 Å and 3.65 Å, respectively). These ion triplets form loose, uniform but slipped stacks along the *c*-axis, as shown in Fig. 5. Thus, the cation-radical in a given ion-triplet unit further faces IBr_2^- anions from adjacent triplet units, in addition to two IBr_2^- anions associated with neighbouring stacks, with the net result being that each cation-radical is residing in a cavity created by six IBr_2^- anions.

(5a)(I$_3$)(solvent)$_x$. This cation-radical salt contains one electron donor cation on a general position, an I_3^- anion on an inversion center, and a second I_3^- anion on a two-fold rotation axis (perpendicular to the long molecular axis). Furthermore, a disordered solvent molecule (modeled as a number of partially occupied Cl and C atoms without regard to a recognizable fragment, but presumed to be TCE) occupies at least partially a void in the crystal structure. The molecule **5a** found in this salt (Fig. 6) has idealized molecular symmetry D_2, and a racemic mixture of both enantiomers is present. As is the case in all crystal structures reported in this paper, the ethyl group substituents are arranged axially with respect to the six-membered ring of the molecule, but the orientation of the methyl groups varies over the four sites, thus breaking the D_2 molecular symmetry. This conformational variability (CH_3–CH_2–CH–ring torsion angle) is likely dictated by packing forces. On the other hand, a preference for axial orientation of ethyl groups is observed in all these compounds, which may be the conformation with the minimal steric energy between adjacent ethyl groups.

The overall structure is layered, with one triiodide anion–solvent slabs separating the layers containing electron donor molecule cations and the second triiodide anion. However, unlike most ET salts,[3a] where the intermolecular interactions within the organic donor layer are dominated by intermolecular S···S and C–H···S contacts, in **(5a)**(I$_3$)(solvent)$_x$, with one of the crystallographically distinct triiodide anions residing in the organic donor molecules layer separating the donor molecules zigzag ribbons along the *b*-direction (see Fig. 7), there exist several short S···I contacts (donor–anion) in addition to the S···S and C–H···S contacts (donor–donor).

(7)$_2$(IBr$_2$)$_3$. This cation-radical salt contains two crystallographically distinct layers of composition (**7**)(IBr_2), one centered around $x \approx 0$ (Layer 1), the other at $x \approx 0.5$ (Layer 2).[24] Separating these mixed layers are layers of disordered IBr_2^- anions at $x \approx \pm 0.25$, see Fig. 8. The triatomic anion can adopt one of two overlapping positions, separated by one I–Br bond length.

Mixed layers with trihalides have been observed in several ET salts, notably ε-$(ET)_2(I_3)(I_8)_{0.5}$,[17a] ζ-$(ET)_2(I_3)(I_5)$,[17b] $(ET)_2(I_3)(TlI_4)$[17b] and $(ET)_2(IBr_2)_2(TCE)_{0.5}$.[18] But in contrast to the ET salts, where there is a 2:1 donor:anion ratio within the layer, in the present compound there is a 1:1 ratio. In layer 2 (Fig. 9) the ethyl group substituents of the electron-donor molecule are fairly well-ordered, and the *trans*-configuration is confirmed. Within the layer, each donor molecule is surrounded by four anions, and *vice versa*. The shortest

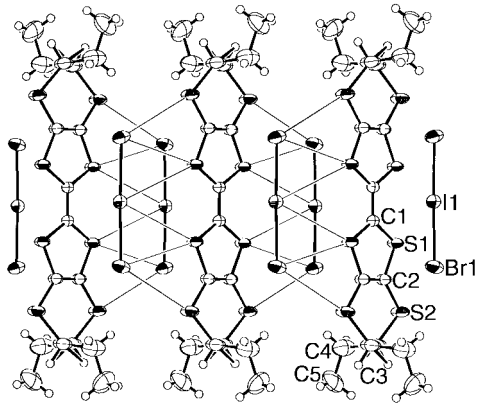

Fig. 5 Stack of ion triplets (see text) in (*meso*-**5a**)(IBr_2)$_2$. The *c*-axis is horizontal. All atoms except hydrogen are drawn with 50% probability thermal ellipsoids.

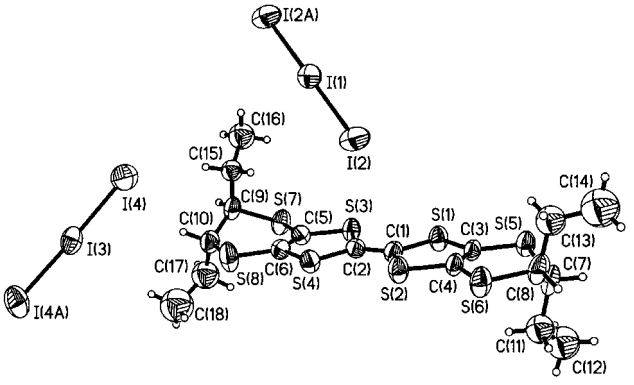

Fig. 6 The electron donor molecule and its neighboring anions in (**5a**)(I$_3$)(solvent)$_x$. All atoms except hydrogen (not labeled) are drawn with 50% probability thermal ellipsoids.

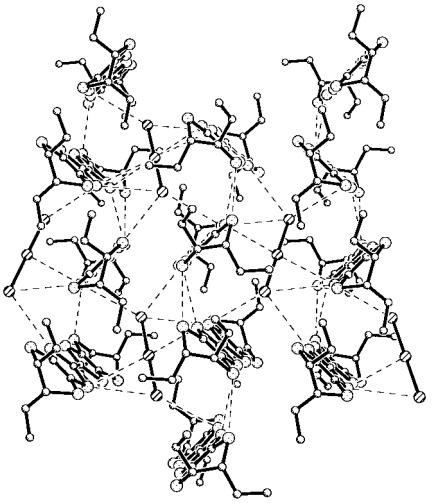

Fig. 7 Mixed donor–anion layer in (**5a**)(I$_3$)(solvent)$_x$. Intermolecular contacts shorter than the sum of the van der Waals radii (1.8 Å for S, 1.98 Å for I) are indicated by thin lines. Hydrogen atoms are omitted for clarity.

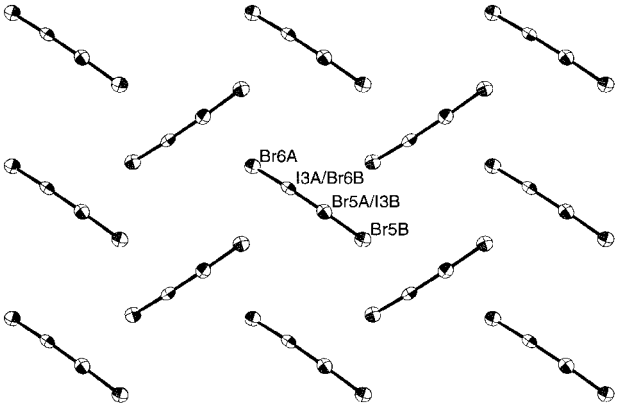

Fig. 8 Disordered anion layer in (**7**)$_2$(IBr_2)$_3$. The terminal atoms were modeled as half-occupied bromine atoms, whereas the central atoms were modeled as a superposition of 50% bromine and 50% iodine.

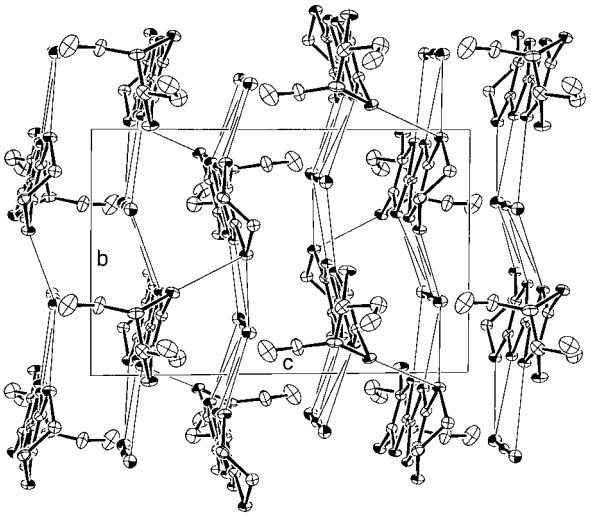

Fig. 9 Mixed donor–anion layer 2 in $(\mathbf{7})_2(IBr_2)_3$. Intermolecular contacts shorter than the sum of the van der Waals radii (1.8 Å for S, 1.85 Å for Br, 1.98 Å for I) are indicated by thin lines. Hydrogen atoms are omitted for clarity.

donor-to-donor intermolecular contact distance is 3.58 Å, essentially the same as the sum of the van der Waals radii, 3.60 Å,[19] but numerous short S···I contacts exist.

The packing of layer 1 is similar to that of layer 2, except that the hexane-3,4-diyl end groups of the diethyl-ET molecules are conformationally disordered. Fig. 10 shows a model of the disordered molecule. The conformational disorder is not found to be synchronized with the disorder of adjacent IBr_2^- groups in the anion layer, based on the differences in site occupancy factors: 0.098(2):0.902(2) for the anion sites and 0.84(2):0.16(2) for the hexane-3,4-diyl groups.

Raman spectroscopy

For the ET electron-donor molecule and its radical cation salts, a linear relationship between the totally symmetric C=C vibrational stretching frequencies and the oxidation state of the donor molecule has been observed recently.[20–23] The ν_2 and ν_3 modes of A_g symmetry are associated with the symmetric C=C stretching vibrations involving atoms with bonding orbitals and large orbital coefficients. The effect of higher oxidation state of the ET molecule in its cation-radical salts is to remove electrons from the bonding orbitals, render the C=C bond more single bond-like, and decrease the C=C vibration frequency.[21,23] The ν_9 A_g mode is associated with the stretching of C–S bonds which are antibonding in nature, and the effect of higher oxidation state is to remove electrons from the antibonding orbitals and increase the C–S stretching frequency. Therefore, based on the Raman shifts, the oxidation state of the ET molecule in a newly prepared ET salt can be rapidly determined.

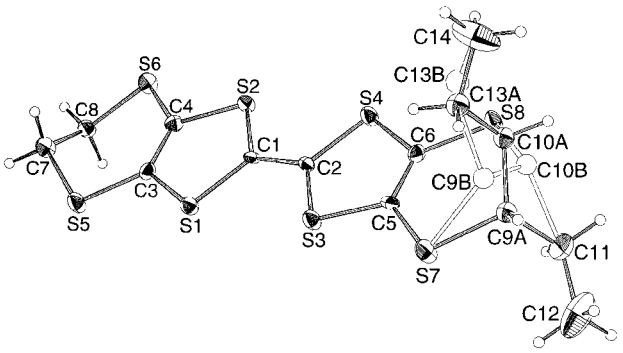

Fig. 10 The disordered electron donor molecule **7** as found in layer 1 of $(\mathbf{7})_2(IBr_2)_3$. No hydrogen atoms were assigned for the minority conformation (outlined atoms and bonds). All non-hydrogen atoms are drawn with 20% probability thermal ellipsoids.

The tetraethyl-ET electron-donor molecule has the same C_6S_8 core, and is expected to show similar vibrational characteristics to those of the ET molecule. Consequently, a correlation between the Raman shifts and the oxidation state of tetraethyl-ET can be expected. We have found this to be the case, and have used this correlation to determine the oxidation state of tetraethyl-ET in one of its cation-radical salts with ClO_4^- as the counterion. The crystals of this salt were too small to be used for X-ray diffraction studies to ascertain its composition and structure.

Raman spectra were measured on crystalline samples of neutral tetraethyl-ET **5a**, and the cation-radical salts $\mathbf{5a}(I_3)(TCE)_x$, $\mathbf{5a}(AuCl_4)(AuCl_2)$, and $\mathbf{5a}(IBr_2)_2$. The Raman spectrum of $\mathbf{5a}(AuCl_4)(AuCl_2)$ is shown in Fig. 11.

As shown in Fig. 11, the four strong scattering peaks can be readily identified as the totally symmetric ν_2, ν_3, ν_6, and ν_9 A_g modes based on the intensity and the observation of the combination modes ($\nu_2+\nu_9$, $\nu_3+\nu_9$ and $\nu_3+\nu_6$) as well as the overtone modes ($2\times\nu_6$ and $2\times\nu_9$ A_g, not labeled). The major Raman peaks of the tetraethyl-ET and its salts are listed in Table 4. The Raman shifts of the tetraethyl-ET salts are a few wavenumbers higher than those of similar ET salts suggesting a stiffer crystal lattice. The stretching frequencies of the ν_2 and ν_3 A_g modes are plotted against the oxidation states of the tetraethyl-ET in Fig. 12.

An approximately linear relationship between the C=C stretching frequency and the oxidation state of tetraethyl-ET is observed. The slopes of the best-fit lines for the ν_2 and ν_3 A_g modes are -91 and $-108\ cm^{-1}$ per unit of oxidation state, respectively, which compare favorably with the corresponding values of -81 and $-104\ cm^{-1}$ per unit of oxidation state in ET salts.[20]

The Raman spectrum was also recorded for a newly prepared salt of **5a** with ClO_4^- anion. This material exhibited an ESR signal with a peak-to-peak line width of 12–18 G, indicating the presence of unpaired electrons. Based on the established correlation in Fig. 12, the observed Raman shifts of 1446 and

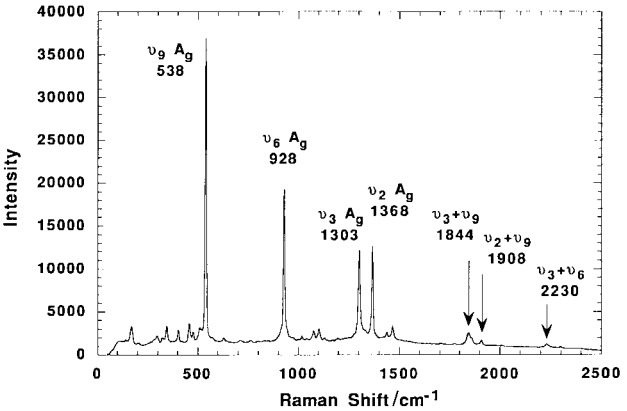

Fig. 11 Raman spectrum of $\mathbf{5a}(AuCl_4)(AuCl_2)$ showing the strong fundamental A_g modes and the combination modes.

Table 4 Raman shifts of the tetraethyl-ET **5a** salts[a]

Compound	$\nu_2 A_g$	$\nu_3 A_g$	$\nu_6 A_g$	$\nu_9 A_g$
ET **8**	1554 m	1497 vs	992 m	488 s
Tetraethyl-ET **5a**	1557 m	1506 vs	995 m	491 w
$\mathbf{5a}(I_3)(TCE)_x$	1458 m	1424 m		509 m
$\mathbf{5a}(ClO_4)$	1446 m	1422 vs	1001 m	514 w
$\mathbf{5a}(AuCl_4)(AuCl_2)$	1368 s	1303 s	928 s	538 vs
$\mathbf{5a}(IBr_2)_2$	1377 vs	1286 s	924 s	527 vs

[a]vs very strong, s strong, m medium, w weak.

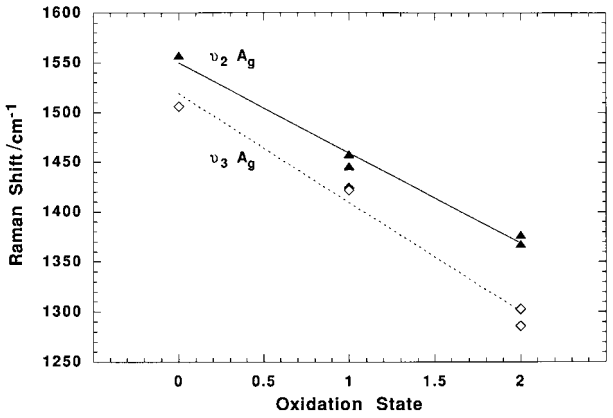

Fig. 12 The ν_2 and ν_3 C=C stretching frequencies of tetraethyl-ET compounds *versus* the oxidation states (0, +1, and +2) showing an approximately linear relationship.

1422 cm^{-1} allowed the unambiguous assignment of the stoichiometry as **5a**(ClO_4), a 1:1 salt, ignoring the possibility of a cocrystallized solvent. Therefore, Raman spectroscopy serves as a convenient tool for the characterization of newly prepared cation-radical salts whose composition cannot be determined by traditional methods such as X-ray diffraction.

Concluding remarks

In this paper, we have described a convenient stereoselective synthesis of dialkyl- and tetraalkyl-ET derivatives *via* the Diels–Alder approach using the readily available trithione oligomer, albeit as racemic mixtures of diastereomers. The most notable finding in our studies is that the cation-radical salts derived from these poly-alkyl derivatives are not of the usual 2:1 donor:anion stoichiometry (nominal oxidation state of the electron-donor molecule = +0.5), found predominantly in the cation-radical salts derived from ET and related electron-donor molecules. The principal reason for the higher oxidation states found in the cation-radical salts of diethyl- and tetraethyl-ET derivatives (+1, +1.5, and +2, see Table 5) is likely to be the increased solubility of the neutral donors and their cation-radical species in the solvents used for crystal growth by electrocrystallization and/or chemical oxidation. This inference is consistent with our unsuccessful attempts thus far to obtain crystals of the cation-radical salts of dipropyl- and tetrapropyl-ET derivatives, which are even more soluble than the corresponding ethyl derivatives.

Secondly, from the crystal structures of solids derived from tetraethyl-ET thus far—both neutral donor and its cation-radical salts—the ethyl groups were found in axial positions. While this is somewhat unexpected, the molecular packing in these solids may be dictated by the intermolecular interactions such as S···S, CH···anion, S···anion interactions, which are stronger and more dominant than the hydrophobic attractive interactions between ethyl groups. However, in view of the facile conformational mobility of the ethanediyl endgroups bearing the alkyl substituents, it is likely that steric (repulsive) interactions between the alkyl groups might force them into the axial configuration. Indeed, there might be a delicate balance between all of these weak intermolecular interactions, and in materials with different donor–anion combinations, we fully anticipate finding cation-radical salts in which the alkyl groups are in equatorial positions.

Thirdly, the usefulness of Raman spectroscopy in ascertaining the oxidation state of the organic electron donor and stoichiometry of cation-radical salt crystals which are too small for X-ray studies, *viz.*, **(5a)**ClO_4, is once again demonstrated in this work.

Finally, as expected for cation-radical salts with donor molecules in the +2 oxidation state, **(5a)**$(AuCl_2)(AuCl_4)$ and (*meso*-**5a**)$(IBr_2)_2$ are insulators (resistivities $> 10^6$ Ω cm). The triodide salt **(5a)**$(I_3)(solvent)_x$ was not sufficiently stable (loss of iodine) to determine its electrical properties. We were able to carry out four-probe measurements on single crystals of $(\mathbf{7})_2(IBr_2)_3$ which was found to be a semiconductor. The conductivity of this salt at 297 K was *ca.* 8.0×10^{-4} S cm^{-1}. Between 297 K and *ca.* 160 K, the temperature dependence of resistivity exhibited activated behaviour with $E_a = 86$ meV; below *ca.* 160 K, there was a steep upturn in resistivity, reaching a value of *ca.* 1.5 MΩ cm at 100 K.

Although the high solubility of the new ET derivatives **5a**, **5b** and **7** has hampered our attempts so far in growing crystalline cation-radical salts with other commonly employed anions such as polymeric anions, the use of less-soluble and electro-active anionic components such as $[Ni(dmit)_2]^{2-}$ is expected to circumvent this problem and to furnish new crystalline conducting solids. Such studies are currently underway in our laboratory.

Experimental

General

Melting points were determined in open capillaries and are not corrected. ^{1}H NMR spectra were recorded at 300 MHz on either Bruker AM-300 or GE Omega 300 spectrometers in $CDCl_3$ containing 0.03% TMS as an internal standard, and the chemical shifts are reported in δ. IR spectra were recorded on a Nicolet 510P FTIR spectrophotometer on KBr pellets. Mass spectra (electron impact ionization) were recorded at the Washington University Resource for Biomedical and Bioorganic Mass spectrometry. Elemental analyses were per-

Table 5 Average bond distances (Å) for **5a** and its cation-radical salts, compared with the cation charge. The calculated charges and δ were obtained from the observed bond lengths by use of the formula in ref. 25

	5a	**(5a)**$I_3(TCE)_x$	**(5a)**$(AuCl_2)(AuCl_4)$	**(5a)**$(IBr_2)_2$	$(\mathbf{7})_2(IBr_2)_3$
Cation charge	0	+1	+2	+2	+1.5
Calc. charge	+0.2	+0.9	+1.6	+1.7	+1.4
δ	0.820	0.733	0.631	0.629	0.662
Central C=C	1.344(5)	1.389(11)	1.44(3)	1.421(14)	1.406(14)
Outer C=C	1.343(6)	1.336(12)	1.34(2)	1.369(12)	1.37(2)
Central C–S	1.751(3)	1.719(9)	1.682(8)	1.697(4)	1.711(11)
5-C–S	1.756(3)	1.740(9)	1.729(11)	1.722(6)	1.730(12)
6-C–S	1.745(3)	1.744(8)	1.737(11)	1.732(6)	1.733(12)
Outer C–S	1.823(4)	1.828(10)	1.84(2)	1.837(8)	1.840(15)
Ethylene C–C	1.522(8)	1.50(2)	1.47(3)	1.45(2)	1.50(2)
Ethyl C–C	1.524(6)	1.55(2)	1.53(3)	1.586(13)	1.52(2)
Terminal C–C	1.504(6)	1.50(2)	1.46(3)	1.489(13)	1.48(3)
Anions	—	2.9152(10)	2.258(5)	2.6876(9)	2.711(2)
	—	(I–I)	(Au–Cl)	(I–Br)	(I–Br)

formed by Midwest Microlab, Indianapolis, Indiana. Cyclic voltammetry (CV) was performed by use of an IBM ec/225 voltammetric analyzer and an IBM 7424 *x–y* recorder. Dichloromethane used for CV was Mallinckrodt HPLC grade. Tetrabutylammonium hexafluorophosphate, used in CV experiments, was recrystallized from ethyl acetate and vacuum dried prior to use. Raman spectra were measured at room temperature on crystalline samples with the use of a Raman microscope spectrometer (Renishaw Ltd.) equipped with a He–Ne laser (6328 Å). A typical spectrum was taken with 0.6 mW laser power and signal-averaged over 20 scans. The oligomeric trithione was synthesized according to literature methods.[11,13] Unless otherwise specified, all other reagents and solvents were used as received.

trans-5,6-Dihydro-5,6-diethyl-1,3-dithiolo[4,5-*b*][1,4]dithiine-2-thione (3a) and *trans*-5,6-dihydro-5,6-dipropyl-1,3-dithiolo[4,5-*b*][1,4]dithiine-2-thione (3b)

To a stirred suspension of oligotrithione **1** (2.0 g, 10.2 mmol) in 200 mL of toluene was added *trans*-hex-3-ene (1.71 g, 20.4 mmol), and the mixture was refluxed under argon for 2 h. The wine-red reaction mixture was passed through a short silica column with a 2:1 mixture of $CHCl_3$–hexane as eluent. Evaporation of the solvent and drying *in vacuo* resulted in a dark wine-red gummy semisolid. Recrystallization from ethanol with charcoal as decolorizing agent afforded 2.19 g (77%) of **3a** as bright yellow needles. Similarly, reaction of **1** (1.5 g, 7.65 mmol) with *trans*-oct-4-ene (1.03 g, 9.20 mmol) in 75 mL of toluene yielded 1.72 g (73%) of **3b** as bright yellow microcrystals.

3a. Mp 77–78 °C; ^{1}H NMR ($CDCl_3$): δ 3.11 (m, 2H), 1.84 (m, 4H), 1.08 (t, 6H, $J=7.3$ Hz); IR (ν/cm^{-1}, KBr) 2963, 2934, 2905, 2872, 2843, 1482, 1458, 1063, 1032, 1012, 793; elemental analysis: calc. for $C_9H_{12}S_5$: C, 38.54; H, 4.31; S, 57.15%. Found: C, 38.58; H, 4.27; S, 57.36%.

3b. Mp 98–99 °C; ^{1}H NMR ($CDCl_3$): δ 3.18 (m, 2H), 1.74 (m, 4H), 1.55 (m, 4H), 1.09 (t, 6H, $J=7.3$ Hz); IR (ν/cm^{-1}, KBr) 2955, 2929, 2900, 2870, 2838, 1632, 1477, 1058, 1031, 1022, 886, 804; elemental analysis: calc. for $C_{11}H_{16}S_5$: C, 42.82; H, 5.23; S, 51.96%. Found: C, 42.86; H, 5.19; S, 52.03%.

trans-5,6-Dihydro-5,6-diethyl-1,3-dithiolo[4,5-*b*][1,4]dithiin-2-one (4a) and *trans*-5,6-dihydro-5,6-dipropyl-1,3-dithiolo[4,5-*b*][1,4]dithiin-2-one (4b)

To a solution of thione **3a** (2.33 g, 8.32 mmol) in 30 mL $CHCl_3$ was added 7.5 mL glacial acetic acid and $Hg(OAc)_2$ (5.27 g, 16.54 mmol) under argon, and the mixture was stirred in the dark at room temperature. After 30 min, the white precipitate was filtered off and washed with $CHCl_3$. The filtrate was then washed with water (4×100 mL), saturated aqueous $NaHCO_3$ (1×100 mL) and water again (1×100 mL). Drying the organic layer (anhydrous $MgSO_4$) and evaporation *in vacuo* afforded 2.13 g (97%) of spectroscopically pure dithiocarbonate **3a** as a yellow semisolid, which can be used directly for the next reaction. Further purification by recrystallization from ethanol with charcoal as decolorizing agent gave 1.58 g (72%) of analytically pure **4a** as cream yellow crystals. Similarly, reaction of **3b** (2.68 g, 8.70 mmol) with $Hg(OAc)_2$ (5.51 g, 17.29 mmol) in 60 mL of 4:1 $CHCl_3$–glacial acetic acid mixture afforded 2.22 g (87%) of spectroscopically pure **4b** as pale yellow crystals (mp 52–53 °C), which can be used directly for the next reaction. Recrystallization from hexane with charcoal as decolorizing agent gave 1.73 g (68%) of analytically pure **4b** as cream yellow crystals.

4a. Mp 73–74 °C; ^{1}H NMR ($CDCl_3$): δ 3.10 (m, 2H), 1.87 (m, 4H), 1.09 (t, 6H, $J=7.3$ Hz); IR (ν/cm^{-1}, KBr) 2963, 2953, 2924, 2870, 1720, 1673, 1628, 1499, 1456, 903, 887, 763; elemental analysis: calc. for $C_9H_{12}OS_4$: C, 40.88; H, 4.57; S, 48.50%. Found: C, 41.04; H, 4.50; S, 48.09%.

4b. Mp 54–55 °C; ^{1}H NMR ($CDCl_3$): δ 3.17 (m, 2H), 1.80 (m, 4H), 1.53 (m, 4H), 0.96 (t, 6H, $J=7.3$ Hz); IR (ν/cm^{-1}, KBr) 2953, 2925, 2893, 2866, 2833, 1697, 1682, 1634, 1499, 1457, 1424, 905, 887, 788; elemental analysis: calc. for $C_{11}H_{16}OS_4$: C, 45.17; H, 5.51; S, 43.85%. Found: C, 45.20; H, 5.33; S, 43.57%.

2-[*trans*-5,6-Dihydro-5,6-diethyl-1,3-dithiolo[4,5-*b*][1,4]dithiin-2-ylidene]-*trans*-5,6-dihydro-5,6-diethyl-1,3-dithiolo[4,5-*b*][1,4]dithiine (5a)

A stirred solution of **4a** (0.69 g, 2.61 mmol) in 3 mL of neat, freshly distilled trimethyl phosphite was refluxed under argon for 7 h. To the dark red reaction mixture was added 20 mL of methanol, and the resulting red precipitate was suction filtered, washed with methanol, dried (*in vacuo*), affording 0.57 g of a red solid (mp 148–150 °C). Recrystallization from 2:1 hexane–$CHCl_3$ yielded 0.48 g (74%) of analytically pure **5a** as deep red crystals.

5a. Mp 179–180 °C (decomp.); ^{1}H NMR ($CDCl_3$): δ 3.03 (p, 4H, $J=5.7$ Hz), 1.73 (m, 8H), 1.04 (t, 12H, $J=7.3$ Hz); IR (ν/cm^{-1}, KBr) 2965, 2932, 2872, 1635, 1455, 1375, 1306, 901, 797, 772; MS *m*/*z* (relative intensity): 496 (85, M^+), 412 (100), 328 (31), 248 (41); elemental analysis: calc. for $C_{18}H_{24}S_8$: C, 43.51; H, 4.87; S, 51.62%. Found: C, 43.47; H, 4.75; S, 51.48%.

2-[*trans*-5,6-Dihydro-5,6-dipropyl-1,3-dithiolo[4,5-*b*][1,4]dithiin-2-ylidene]-*trans*-5,6-dihydro-5,6-dipropyl-1,3-dithiolo[4,5-*b*][1,4]dithiine (5b)

A stirred solution of **4b** (0.50 g, 1.71 mmol) in 3 mL of neat, freshly distilled trimethyl phosphite was refluxed under argon for 7 h. During this time the reaction mixture turned dark red. Excess trimethyl phosphite was distilled off under vacuum. Column chromatography (silica gel, 230–400 mesh; hexane–$CHCl_3$, 10:1 v/v) of the brown red residue gave a pink red semisolid; which upon trituration with hexanes and drying (*in vacuo*) yielded 0.33 g (70%) of analytically pure sample of **5b**.

5b. Mp 62–63 °C; ^{1}H NMR ($CDCl_3$): δ 3.09 (t, 4H, $J=$ 5.6 Hz), 1.74 (m, 4H), 1.65 (m, 4H), 1.56 (m, 4H), 1.42 (m, 4H), 0.93 (t, 12H, $J=7.3$ Hz); IR (ν/cm^{-1}, KBr) 2956, 2928, 2869, 1653, 1523, 1459, 1434, 1185, 1101, 1079, 999, 885, 771; MS *m*/*z* (relative intensity): 522 (9, M^+), 481 (5), 440 (22), 410 (44), 386 (55), 368 (47), 341 (100); elemental analysis: calc. for $C_{22}H_{32}S_8$: C, 47.78; H, 5.83; S, 46.39%. Found: C, 48.04; H, 5.71; S, 46.20%.

2-[*trans*-5,6-Dihydro-5,6-diethyl-1,3-dithiolo[4,5-*b*][1,4]dithiin-2-ylidene]-5,6-dihydro-1,3-dithiolo[4,5-*b*][1,4]dithiine (7)

Condition 1. Trithiocarbonate **6** (0.25 g, 1.11 mmol) and dithiocarbonate **4a** (0.25 g, 0.95 mmol) were suspended in 2 mL of neat, freshly distilled trimethyl phosphite under argon. The mixture was refluxed for 5 h during which a red precipitate was formed. After removal of excess of trimethyl phosphite under vacuum, the residue was purified by column chromatography (silica gel, 230–400 mesh; hexane–CS_2, 1:2 v/v). The second orange–yellow fraction was collected, evaporated, dried to give 100 mg (24%) of spectroscopically pure **7** as yellow crystalline solid (mp 129–130 °C). The first and third fractions yielded **5a** (50 mg) and **8** (70 mg)

respectively, resulting from the homocoupling reaction. Recrystallization of **7** from $CHCl_3$–hexane mixture yielded 75 mg of analytically pure sample as pale orange–yellow fluffy needles (mp 131–132 °C).

Condition 2. Trithiocarbonate **6** (0.25 g, 1.11 mmol) and dithiocarbonate **4a** (0.25 g, 0.95 mmol) were suspended in 3 mL of freshly distilled toluene and 0.78 mL of freshly distilled trimethyl phosphite under argon. The mixture was refluxed for 7 h during which a red precipitate was formed. After removal of toluene and excess of trimethyl phosphite under vacuum, the residue was purified by column chromatography as above (Condition 1) yielding 60 mg (14%) of spectroscopically pure **7** as an orange–yellow crystalline solid (mp 129–130 °C). The first and third fractions yielded **5a** (10 mg) and **8** (20 mg) respectively, resulting from the homocoupling reaction.

Condition 3. Trithiocarbonate **6** (124 mg, 0.55 mmol) and dithiocarbonate **4a** (125 mg, 0.47 mmol) were suspended in 1.5 mL of trimethyl phosphate and 0.39 mL of neat, freshly distilled trimethyl phosphite under argon. The mixture was refluxed for 6 h during which a red precipitate was formed. After removal of excess of trimethyl phosphite under vacuum, the residue was purified by column chromatography as above (Condition 1) yielding 50 mg (24%) of spectroscopically pure **7** as an orange–yellow crystalline solid (mp 129–130 °C). The first and third fractions yielded **5a** (20 mg) and **8** (16 mg) respectively, resulting from the homocoupling reaction.

Condition 4. Dithiocarbonate **9** (0.47 g, 2.26 mmol) and trithiocarbonate **3a** (0.66 g, 2.36 mmol) were suspended in 4.5 mL of neat, freshly distilled trimethyl phosphite under argon. The mixture was refluxed for 6 h. Employing work up conditions as mentioned above (Condition 1) yielded 0.35 g (35%) of spectroscopically pure **7** as an orange–yellow crystalline solid (mp 130–132 °C). The first and third fractions yielded **5a** (0.12 g) and **8** (0.2 g) respectively, resulting from homocoupling reaction.

7. ^{1}H NMR ($CDCl_3$): δ 3.29 (s, 4H), 3.03 (m, 2H), 1.75 (m, 4H), 1.05 (t, 6H, $J=7.5$ Hz); IR (ν/cm^{-1}, KBr) 2959, 2929, 2872, 2845, 1505, 1456, 1448, 1370, 1298, 1285, 1130, 912, 873, 788, 772; MS m/z (relative intensity): 440 (73, M^+), 412 (6), 356 (100), 192 (38); elemental analysis: calc. for $C_{14}H_{16}S_8$: C, 38.18; H, 3.64; S, 58.18%. Found: C, 38.31; H, 3.41; S, 57.96%.

Preparation of cation-radical salts

For the preparation of (**5a**)($AuCl_4$)($AuCl_2$), (**5a**)(IBr_2)$_2$ and (**5a**)ClO_4, standard H-cells equipped with Pt electrodes were used for electrocrystallization. For the ($AuCl_4$)($AuCl_2$) salt, in the anode compartment 5 mg of **5a** and 40 mg (*ca.* 6 equivalents) of PPh_4AuCl_4 were placed, and in the cathode compartment 40 mg of PPh_4AuCl_4 were placed. Freshly distilled 1,1,2-trichloroethane (TCE), *ca.* 7.5 mL, was added to both sides. For the IBr_2 salt: 9 mg of **5a** in anode compartment; 72 mg (*ca.* 7.5 equivalents) of NBu_4IBr_2 and 7.5 mL of freshly distilled tetrahydrofuran (THF) in each compartment. For the ClO_4 salt: 8 mg of **5a** in the anode compartment; 41 mg (*ca.* 7.5 equivalents) of Bu_4NClO_4 and 7.5 mL of chlorobenzene in each compartment. In each case, the initial current density was set at 0.2 μA cm^{-2} and was slowly increased by 0.25 μA increments every two days as long as there was no crystal nucleation. Once the nucleation commenced, the crystals were allowed to grow for an additional two weeks before they were harvested.

The triiodide salt of **5a** was prepared by slow diffusion of iodine vapors from a solution of I_2 (32 mg) in 0.5 mL of TCE in to a solution of **5a** (10 mg) in 5 mL of TCE. Black shiny crystals of the salt were harvested after two days.

Acknowledgements

This work was supported by the U.S. Department of Energy, Office of Basic Energy Sciences, Division of Materials Science, under Contract W-31-109-ENG-38. F.R., E.D., and S.T. were undergraduate research participants sponsored by the Argonne Division of Educational Programs from the University of Puerto Rico-Cayey, Cayey, PR, College of the Holy Cross, Worcester, MA, and Williams College, Williamstown, MA, respectively. Mass spectrometry data were provided by the Washington University Mass Spectrometry Resource which was supported by NIH (Grant #P41RR0954).

References

1 See *e.g.*, Special Issue on Molecular Conductors, *J. Mater. Chem.*, 1995, **10**, 1469.
2 L. G. Caron, in *Organic Conductors—Fundamentals and Applications*, ed. J.-P. Farges, Marcel-Dekker, New York, 1994, Ch. 2, pp. 25–73.
3 (*a*) J. M. Williams, J. R. Ferraro, R. J. Thorn, K. D. Carlson, U. Geiser, H. H. Wang, A. M. Kini and M.-H. Whangbo, *Organic Superconductors (Including Fullerenes)*, Prentice Hall, Englewood Cliffs, NJ, 1992; (*b*) T. Ishiguro and K. Yamaji, *Organic Superconductors*, Springer-Verlag, Berlin Heidelberg, 1990.
4 (*a*) J. Hellberg, K. Balodis, M. Moge, P. Korral and J.-U. von Schütz, *J. Mater. Chem.*, 1997, **7**, 31; (*b*) J. Yamada, S. Mishima, H. Anzai, M. Tamura, Y. Nishio, K. Kajita, T. Sato, H. Nishikawa and K. Kikuchi, *Chem. Commun.*, 1996, 2517; (*c*) Y. Misaki, T. Ohta, N. Higuchi, H. Fujiwara, T. Yamabe, T. Mori, H. Mori and S. Tanaka, *J. Mater. Chem.*, 1995, **5**, 1571; (*d*) A. J. Moore, M. R. Bryce, D. J. Ando and M. B. Hursthouse, *J. Chem. Soc., Chem. Commun.*, 1991, 320; (*e*) T. K. Hansen, M. V. Lakshmikantham, M. P. Cava and J. Becher, *J. Chem. Soc., Perkin Trans. 1*, 1991, 2873.
5 (*a*) J. D. Wallis, A. Karrer and J. D. Dunitz, *Helv. Chim. Acta*, 1986, **69**, 69; (*b*) A. I. Kotov, C. Faulmann, P. Cassoux and E. B. Yagubskii, *J. Org. Chem.*, 1994, **59**, 2626.
6 A. M. Kini, U. Geiser, H. H. Wang, K. R. Lykke, J. M. Williams and C. F. Campana, *J. Mater. Chem.*, 1995, **5**, 1647.
7 J. P. Parakka, A. M. Kini and J. M. Williams, *Tetrahedron Lett.*, 1996, **37**, 8085.
8 J. M. Williams, *Mol. Cryst. Liq. Cryst.*, 1996, **284**, 449.
9 (*a*) C. Benming, F. Deilacher, M. Hoch, H. J. Keller, P. Wu, P. Armbruster, R. Geiger, S. Kahlich and D. Schweitzer, *Synth. Met.*, 1991, **42**, 2101; (*b*) S. Matsumiya, A. Izuoka, T. Sugawara, T. Taruishi and Y. Kawada, *Bull. Chem. Soc. Jpn.*, 1993, **66**, 513.
10 J. S. Zambounis, C. W. Mayer, K. Hauenstein, B. Hilti, W. Hofher, J. Pfeiffer, M. Bürkle and G. Rihs, *Adv. Mater.*, 1992, **4**, 33.
11 (*a*) O. Neilands, J. Kaicens and J. Kreicberga, USSR Patent #SU 1428753, 1988; *Chem. Abstr.*, 1989, **110**, 95252k; (*b*) O. Neilands, J. Kacens and J. Kreicberga, *Zh. Org. Khim.*, 1989, **25**, 658.
12 V. Y. Khodorkovsky, J. Y. Becker and J. Bernstein, *Synthesis*, 1992, 1071.
13 Review: N. Svenstrup and J. Becher, *Synthesis*, 1995, 215.
14 Subsequent to the completion of our synthesis of tetraethyl-ET and tetra(*n*-propyl)-ET, a report appeared in the literature on the Diels–Alder reaction between the trithione oligomer and *trans*-stilbene, see D.-Y. Noh, H.-J. Lee, J. Hong and A. E. Underhill, *Tetrahedron Lett.*, 1996, **42**, 7603.
15 T. Mori and H. Inokuchi, *Chem. Lett.*, 1986, 2069.
16 (*a*) K. A. Abboud, M. B. Clevenger, G. F. de Oliviera and D. R. Talham, *J. Chem. Soc., Chem. Commun.*, 1993, 1560; (*b*) L.-K. Chou, M. A. Quijada, M. B. Clevenger, G. F. de Oliviera, K. A. Abboud, D. B. Tanner and D. R. Talham, *Chem. Mater.*, 1995, **7**, 530.
17 (*a*) R. P. Shibaeva, R. M. Lobkovskaya, É. B. Yagubskii and E. É. Kostyuchenko, *Kristallografiya*, 1986, **31**, 455 (*Engl. Transl. Sov. Phys. Crystallogr.*, 1986, **31**, 267); (*b*) M. A. Beno, U. Geiser, K. L. Kostka, H. H. Wang, K. S. Webb, M. A. Firestone, K. D. Carlson, L. Nuñez, M.-H. Whangbo and J. M. Williams, *Inorg. Chem.*, 1987, **26**, 1912.
18 H. Yamochi, H. Urayama, G. Saito, K. Oshima, A. Kawamoto and J. Tanaka, *Chem. Lett.*, 1988, 1211.

19 A. Bondi, *J. Phys. Chem.*, 1964, **68**, 441.
20 H. H. Wang, J. R. Ferraro, J. M. Williams, U. Geiser and J. A. Schlueter, *J. Chem. Soc., Chem. Commun.*, 1994, 1893.
21 H. H. Wang, A. M. Kini and J. M. Williams, *Mol. Cryst. Liq. Cryst.*, 1996, **284**, 211.
22 R. Swietlik, C. Garrigou-Lagrange, C. Sourisseau, G. Pages and P. Delhaès, *J. Mater. Chem.*, 1992, **2**, 857.
23 J. E. Eldridge, Y. Xie, H. H. Wang, J. M. Williams, A. M. Kini and J. A. Schlueter, *Spectrochim. Acta*, *Part A*, 1996, **52**, 45.
24 The diffraction data for this crystal structure exhibit a strong sublattice with $h+l=2n$, corresponding to a pseudotranslation of $0.5a+0.5c$. The average intensity of the sublattice reflections is approximately ten times that of the $h+l=2n+1$ reflections. However, we have carefully verified from the raw data that the weak reflections are truly present and are not an artefact of detector fluctuations. If the pseudotranslation were exact, the two donor molecule layers would be crystallographically equivalent. In the full unit cell, the main differences are in the conformation and disorder (layer 1) of the ethyl groups.
25 P. Guionneau, C. J. Kepert, G. Bravic, D. Chasseau, M. R. Truter, M. Kurmoo and P. Day, *Synth. Met.*, 1997, **86**, 1973.

Paper 8/09132C